Electron paramagnetic resonance and an optical investigation of photorefractive vanadium-doped CdTe

Robert N. Schwartz
Hughes Research Laboratories, Malibu, California 90265

Mehrdad Ziari
Center for Photonic Technology, Department of Electrical Engineering, University of Southern California, Los Angeles, California 90089-0483

Sudhir Trivedi
Brimrose Corporation of America, 7720 Belair Road, Baltimore, Maryland 21236
(Received 8 July 1993)

Electron paramagnetic resonance (EPR), photo-EPR, optical absorption, and photoluminescence measurements have been made on photorefractive vanadium-doped CdTe. This EPR observation of the V^{3+} ion in CdTe, along with the observed features assigned to V^{2+} in the optical-absorption spectrum, provide direct evidence for the substitutional incorporation of vanadium. Photo-EPR measurements were also conducted and provide direct evidence for the optical activity of V^{3+} under sub-band-gap illumination. A qualitative discussion linking these observations to photoionization channels is presented.

I. INTRODUCTION

The photorefractive effect has been extensively studied due to its potential uses in a wide range of applications, which include distortion correction and laser power combining via phase conjugation, as well as optical computing and signal processing devices such as reconfigurable optical interconnects and associative memories.[1] To date, because of their large electro-optic properties, the majority of experimental and theoretical work on the physics and applications of the photorefractive effect has been carried out on ferroelectric oxide materials.[1] More recently, however, interest in electro-optic semiconductors as photorefractive materials has grown since these electronic materials exhibit high sensitivity, high speed, and offer the ability to be suitably tailored by well-established band-gap engineering techniques to obtain large optical nonlinearities at any desired wavelength in the infrared spectral region.[2]

It has been known for some time that CdTe, with its large electro-optic coefficient, small dielectric constant, large carrier mobility, and availability in semi-insulating form, has the potential to be a good infrared photorefractive semiconductor.[3] Blysma *et al.*[4] reported the observation of the photorefractive effect in semi-insulating vanadium-doped cadmium telluride (CdTe:V) using an illumination wavelength of 1.06 μm. More recent studies[5,6] showed that efficient photorefractive two-wave coupling energy transfer in CdTe:V occurs also at 1.3- and 1.5-μm wavelengths which are technologically important for optical communications and eye-safe applications. The comparison of the measured photorefractive sensitivity of CdTe:V to other semiconductors and oxides indicated that CdTe:V provides the most sensitive photorefractive response reported to date.[5,7] These studies provided the experimental basis for regarding vanadium as a suitable dopant for introducing *deep levels* that take part in the photorefractive process. In contrast, a recent report[8] of the photorefractive effect in CdTe:V has raised questions regarding the assumed role of vanadium and has disputed its optical activity in the photorefractive process in their samples.

In addition to CdTe:V, there has also been an increased interest in the development of other vanadium-doped photorefractive II-VI compounds[7,9] such as ZnTe and the ternary alloy $Cd_xZn_{1-x}Te$. In order to further advance device development based on vanadium-doped II-VI semiconductors, a thorough understanding of the electronic structure (i.e., charge state and local symmetry) of incorporated vanadium and its relation to the observed deep levels, charge compensation mechanisms, optical absorption, electrical, and photoconductive properties must be established. Due to the extremely high resistivity of photorefractive semiconductors, conventional electrical characterization methods (i.e., deep-level transient spectroscopy) that require contacts are difficult to utilize and/or interpret reliably. Toward this end we have carried out electron paramagnetic resonance (EPR) and photo-EPR measurements on single-crystal CdTe:V. Optical absorption and extensive photorefractive measurements[5,6,10] have also been made on the same crystalline sample. In this paper we will treat the EPR data in depth and correlate them with the observed optical-absorption and photoluminescence data. Only the pertinent results of the photorefractive measurements will be presented here; the details of these measurements and their interpretation will be described in another paper.

This paper is organized as follows. In Sec. II the experimental techniques and procedures are described. Section III presents the main body of the results, i.e., EPR and photo-EPR measurements, optical-absorption data, and identification of optical transitions based on simple

0163-1829/94/49(8)/5274(9)/$06.00

crystal-field theory, and pertinent steady-state two-wave mixing energy coupling results. A general discussion of the results is given in Sec. IV with a comparison with literature data. A summary and conclusion are provided in Sec. V.

II. EXPERIMENTAL PROCEDURES

Vanadium-doped CdTe boules were grown by the modified Bridgman technique. In this method the ampoule and furnace are kept stationary while the temperature profile of the furnace is computer controlled by resistive heating in a predetermined manner. Crystalline material was grown in a pretreated ~1-cm-diam by ~8-cm-long fused silica growth ampoule which contained ~10–15 gm of total charge and sealed under vacuum. The end opposite to the sealed end of the growth ampoule had a conical tip to facilitate nucleation. The starting materials, Cd (99.9999%) and Te (99.9999%), were purified further by repeated sublimation in vacuum (10^{-6}). Metallic vanadium was weighed for a starting concentration of 10^{19} cm^{-3} in the melt and added to a stoichiometric mixture of purified Cd and Te. The charge was initially reacted at 500 °C for about 3 h and then slowly raised to 950 °C, where it was held for 12 h to drive the reaction to completion. The temperature of the charge was then slowly increased at a rate of 1 °C/h to 1120 °C and allowed to mix in the molten state for 48 h. During this phase of the process the temperature of the conical tip was lowered by 10 °C in order to prevent the loss of growth material by sublimation. The furnace temperature was then lowered at a rate of 3 °C/h until the temperature reached 950 °C, where the sample was annealed for 48 h. Finally, the temperature of the furnace was brought to room temperature at a rate of 1 °C/min.

EPR spectra were recorded with a Varian E-109 homodyne X-band spectrometer equipped with a Bruker model B-H15 digital magnetic-field controller. The external magnetic field was modulated at 25 kHz with a modulation amplitude in the range of 1–2 G. The frequency of the spectrometer was measured with a Hewlett-Packard 5342 automatic microwave-frequency counter and a proton magnetic resonance gaussmeter was used to accurately measure the magnetic field. The spectrometer was interfaced to a PC microcomputer for data acquisition and control. Each spectrum was obtained after multiple scans to achieve a satisfactory signal-to-noise ratio. For measurements at low temperatures, an Oxford Instruments ESR-9 continuous-flow helium cryostat system was used. The sample was directly illuminated in the rectangular TE_{102} microwave resonant cavity by means of an optical fiber. The optical fiber was threaded through a 2-mm-i.d. Spectrosil synthetic fused quartz tube which was used to support the crystal sample. The cleaved end of the optical fiber was located approximately 1–2 mm from the crystal. The crystal could be rotated in the magnetic field **B** with the rotation axis parallel with the microwave magnetic field $\mathbf{B}_{mw}$ ($\mathbf{B}_{mw} \perp \mathbf{B}$). Continuous illumination with 1.319-μm light was provided by a Lightwave Electronics model 122 diode-pumped Nd:YAG (yttrium aluminum garnet) laser. The maximum intensity at the sample was approximately 75 mW. A Coherent CR-18 argon-ion laser operating at 514.5 nm was also used to illuminate the crystal in the microwave cavity. The incident power at this wavelength, which is highly absorbed at the surface of the CdTe:V sample, could be varied over the range 50–700 mW.

Optical-absorption spectra were recorded at room temperature using a Cary 2400 spectrophotometer. Photoluminescence (PL) measurements were performed at ~5 K using argon-ion 514.5-nm excitation which was incident on the sample in a near-backscattering geometry. The emitted luminescence was focused onto the entrance slit of a 1-m grating spectrometer. The PL signal was detected using a cooled photomultiplier tube (S1 type) or Ge detector in conjunction with a lock-in amplifier. A PC microcomputer was used for data acquisition and spectrometer wavelength control.

III. RESULTS

A. EPR

No EPR spectrum was observed at room temperature in CdTe:V; however, as the temperature was lowered to about 77 K, a spectrum consisting of eight broad lines was observed centered about the $g \approx 2$ spectral region. Upon further cooling the spectral features sharpened up and additional superhyperfine structure was easily resolved on each line. Near liquid-helium temperatures the observed EPR signal was microwave power sensitive and it was found that powers of about 0.8 mW gave spectra with the optimum signal-to-noise ratio. Shown in Fig. 1 is the EPR spectrum of vanadium-doped CdTe measured at 5 K. The eight lines are the vanadium signature corresponding to the electron-nuclear hyperfine interaction involving the ^{51}V ($I = \frac{7}{2}$, 99.75% natural abundance) nuclide. The observed spectrum is isotropic and can be

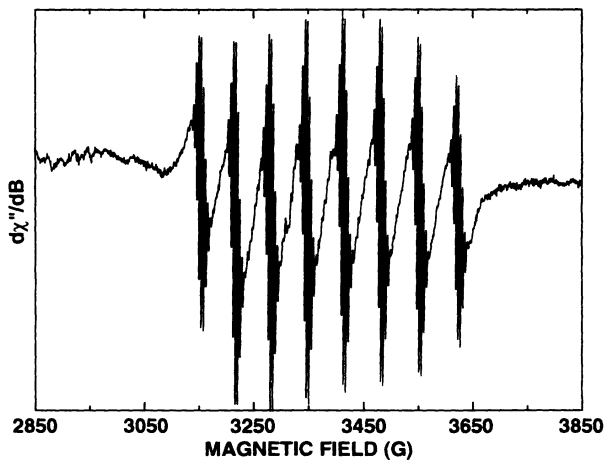

FIG. 1. EPR spectrum of CdTe:V recorded at 5 K. The external magnetic field $\mathbf{B}_0$ is parallel to the [001] direction. The instrumental parameters are microwave frequency $\nu = 9.265\,85$ GHz, microwave power ~0.8 mW, and modulation amplitude = 2 G.

described by a spin Hamiltonian of the form[11]

$$\mathcal{H}=g\beta\mathbf{B}\cdot\mathbf{S}+\mathcal{A}_V\mathbf{S}\cdot\mathbf{I}\ , \quad (1)$$

where the first term describes the Zeeman splitting of the lowest energy levels and the second term describes the hyperfine interaction involving the nuclear spin of ^{51}V. The measured g factor and ^{51}V hyperfine constant $\mathcal{A}_V$ are reported in Table I. The separation between superhyperfine components is 4.35 G; the origin of this structure is discussed below. Continuous illumination in the microwave cavity with either 514.5-nm or 1.319-μm light at 7 K leads to a reduction of the EPR spectrum without changes in the g factor, hyperfine splittings, line shape, or linewidth. Furthermore, no new spectral features were observed under illumination with the available optical irradiance, which is estimated to be on the order of ~ 1 W/cm^2 at the crystal surface for both wavelengths.

B. Optical absorption and photoluminescence

The optical-absorption spectrum of CdTe:V measured at room temperature is shown in Fig. 2. The spectrum was obtained from the measured transmission data corrected for Fresnel reflection, based on the published values of refractive indices.[12] The transitions assigned to V^{2+} intra-3d excitations (crystal-field excitations) from the $^4T_1(^4F)$ ground state to the excited states $^4A_2(^4F)$, $^2E(^2G)$, and $^4T_1(^4P)$ are also indicated in Fig. 2. The values for the excitation energies were taken from the crystal-field analysis of Slodowy and Baranowski[13] who carried out low-temperature (80 K) measurements on CdTe:V. It should be pointed out that there is an expected shift in the absorption features to shorter wavelengths due to the increase in the band-gap energy as the temperature is lowered. The band-gap shift depends on the value chosen for $-dE_g/dT$; however, corrections were found unnecessary because the absorption measurements of Baranowski, and co-workers[14,15] at 80 K are in good agreement with the theoretical values at the same temperature.

TABLE I. g factors and ^{51}V hyperfine coupling constants for substitutional V^{2+} and V^{3+} in semiconductors.

Host:Ion	g factor	^{51}V hyperfine coupling (10^{-4} cm^{-1})	Reference
ZnS:V^{3+}	1.9433	63.0	28
ZnSe:V^{3+}	1.9483	61.3	29
ZnTe:V^{3+}	1.917	57.8	30
CdS:V^{3+}	1.93	63.0	30
CdTe:V^{3+}	1.9549	60.3	This work
GaAs:V^{3+}	1.957	~54–55	31,43
InP:V^{3+}	1.96	55	32
Si:V^{2+}	1.9892	42.1	33
ZnS:V^{2+}	1.961(‖)	40.3(‖)	34
	1.913(⊥)	49.0(⊥)	
$[N(C_4H_9)_4]\cdot(VCl)_4$	1.950(‖)	155(‖)	35
	1.911(⊥)	159(⊥)	

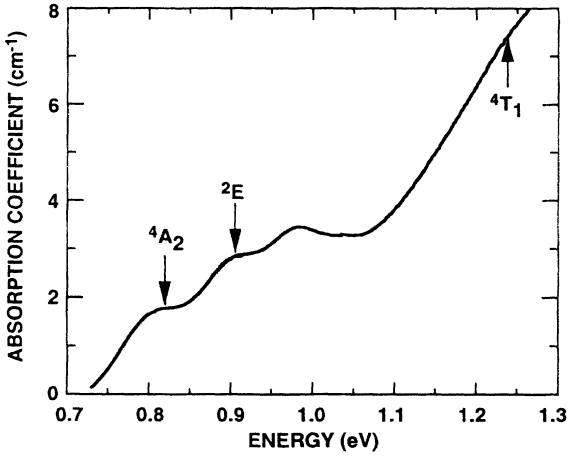

FIG. 2. Optical-absorption spectrum of CdTe:V recorded at room temperature. The positions of the crystal-field transition energies at 80 K are indicated by arrows.

Photoluminescence measurements were made at low temperatures on single-crystalline CdTe:V. The sample surfaces were cleaned with a bromine-methanol solution. It should be pointed out that the sample measured was different from the one used for EPR, optical absorption, and photorefractive gain studies. Shown in Fig. 3 is a representative spectrum in the near-infrared. The broad group of emission peaks centered at approximately 1.45 eV has been extensively studied; however, the exact nature of the defect center responsible for this emission is still a matter of speculation.[16,17] The zero-phonon recombination occurs at ~ 1.458 eV and is followed by a set of phonon replicas separated by the $\mathbf{k}=\mathbf{0}$ longitudinal optical-phonon energy of ~ 0.021 eV. The origin of the peak at 1.496 eV is still unknown, however it has been speculated to involve a transition from a shallow donor level to an acceptor level located at ~ 0.1 eV above the valence-band maximum.[18]

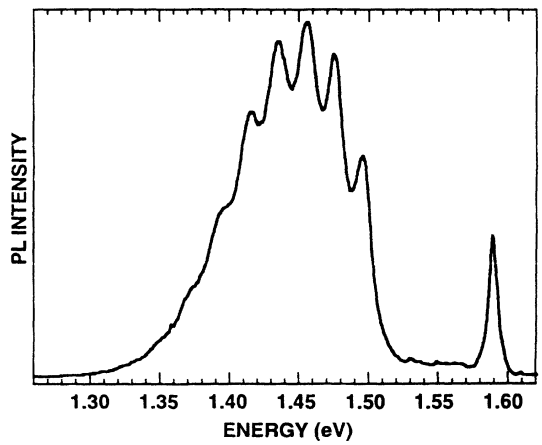

FIG. 3. Near band-edge photoluminescence spectrum of CdTe:V recorded at 5 K.

Another important aspect of the observed PL spectrum from our CdTe:V sample is that the features associated with an oxygen-related center are absent.[19] This is important because Hoang and Baranowski[15] questioned their earlier assignment and suggested that their spectral data may contain features due to an oxygen-related center. It was speculated that oxygen and other impurities were present in the vanadium.

C. Photorefractive measurements

Photorefractive two-beam coupling measurements were made on two samples from the same boule. The experimental conditions and results on the sample used for EPR studies (sample No. 1) were reported in earlier publications.[5,6] In summary, two p-polarized beams interfered on the {110} plane, resulting in a grating along the {100} direction. The intensity gain, defined as the ratio of the detected power of the weak beam in the presence of the strong pump beam to that in the absence of the pump beam, was measured as a function of the grating period (or crossing angle). An iterative nonlinear curve-fitting technique using the Levenberg-Marguard method[20] was applied to the data to provide the important material parameters, namely, the effective trap density N_E and the ξr_{41} product, where r_{41} is the electro-optic coefficient and ξ is the electron-hole competition factor. It was assumed, as is usually done for semiconductors,[21] that the electron-hole competition factor is independent of the grating period. The fitting values for sample No. 1 are $N_E = 5\times10^{15}$ cm^{-3} and $\xi r_{41} = 4.3$ pm/V, which, considering our measured values[5,10] and those in the literature[22] for r_{41}, suggest $|\xi|$ to be close to unity. More recent measurements[6] conducted during field-enhancement experiments on this sample confirm that the same fitting holds at the 1.32-μm wavelength.

An electro-optic identification of the photorefractive carrier (i.e., the sign of ξ) helps to identify the nature of the defect center (i.e., donor or acceptor). In this method, the photorefractive crystal is used as a transverse electro-optic modulator and the sign of the index change is noted using a variable wave plate with known slow and fast axes.[23] A knowledge of the polarity of the applied field with respect to the direction of beam coupling, along with the sign of the index change, is sufficient to determine the sign of ξ. Our experiments were performed on another sample from the same boule (sample No. 2). However, the ξr_{41} value of the two samples from this boule were identical[6,10] and the findings regarding ξ should equally apply to sample No. 1 used for the EPR studies. Measurements at 1.06-μm wavelength revealed that electrons are the dominant photorefractive carrier (i.e., $\xi<0$). As a safeguard, we checked the setup and procedure against GaAs:Cr and GaAs:*EL*2 samples with known signs of ξ. Furthermore, the relative direction of the beam coupling, and therefore the dominant carrier (electrons), remained the same as the wavelength was changed to 1.32 and 1.5 μm. The significance of these findings to the optical studies of CdTe:V is that the electron domination of the photorefractive process supports the assumed role of vanadium as a deep donor center.

IV. DISCUSSION

A. V^{2+} and V^{3+} electronic properties

The optical and magnetic properties of transition-metal deep impurities in ionic solids[24] and semiconductors[25] are intimately connected with the electronic structure of the embedded ions. As indicated above, the observed optical spectrum in CdTe:V is assigned to V^{2+}, whereas only the V^{3+} ion is seen by EPR. It is only natural to question why the EPR of V^{2+} is not observed in CdTe:V, since it is a paramagnetic $3d^3$ ion and has, for example, been extensively studied in ionic solids.[11] Likewise, the optical absorption of V^{3+} is well studied in ionic solids[26] and III-V semiconductors,[27] and should be discernible in CdTe:V.

If we assume that both ions enter substitutionally without distorting the local T_d point-group symmetry, then straightforward group-theoretical arguments[24] indicate that for the high-spin configuration $e^2t_2^1$ ($3d^3$, $S=\frac{3}{2}$), the ground electronic term for V^{2+} is $^4T_1$, whereas for the low-spin configuration $e^3t_2^0$ ($3d^3$, $S=\frac{1}{2}$), the ground term is ^2E. For the case of V^{3+}, which has the same configuration whether it is low or high spin, i.e., $e^2t_2^0$ ($3d^2$, $S=1$), the ground term is $^3A_2$. From the threshold of the CdTe:V photoconductivity spectrum measured at 80 K, Baranowski, Langer, and Stepanova[14] were able to establish the position of the (V^{2+}/V^{3+}) ionization level relative to the conduction-band minimum, i.e., $E_{CB}-E_{(V^{2+}/V^{3+})}=0.78$ eV. Figure 4 depicts the relative positions of the (V^{2+}/V^{3+}) and (V^{3+}/V^{4+}) ionization levels in the band gap of CdTe:V as well as the $d\rightarrow d^*$ internal transitions for the V^{2+} and V^{3+} ions. It should be pointed out that the position of the (V^{3+}/V^{4+}) ionization level has not been experimentally determined in CdTe:V. The position shown for the (V^{3+}/V^{4+}) level

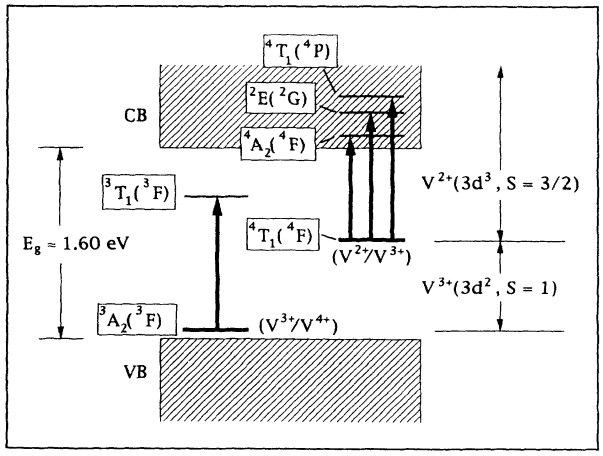

FIG. 4. Combined energy-level diagram showing $d\rightarrow d^*$ internal transitions and ionization levels of substitutional V in CdTe. The thick horizontal lines denote ionization levels, e.g., (V^2/V^{3+}) denotes the position of the Fermi level below which is the V^{3+} charge state and above which is the V^{2+} charge state. Internally excited *d* states of a fixed charge state are denoted by thin horizontal lines.

in Fig. 4 is only approximate and is based on data obtained from optical studies in vanadium-doped III-V semiconductors which are discussed in more detail below.

B. EPR

As pointed out above, the observed hyperfine octet is characteristic of ^{51}V ($I=\frac{7}{2}$). The fact that the observed EPR spectrum is isotropic supports the view that the vanadium dopant enters the CdTe lattice (sphalerite structure, $F\bar{4}3m=T_d^2$) substitutionally while preserving the local cubic symmetry. By comparison with the spin Hamiltonian parameters listed in Table I for V^{2+} and V^{3+} in various crystalline hosts, we assign the observed EPR spectrum in CdTe:V to the V^{3+} ion. The reduction of the ^{51}V hyperfine constant from its value in ionic materials[35] (see Table I) indicates substantial covalency.

The values for the spin Hamiltonian parameters, i.e., g and $\mathcal{A}_V$, were obtained from the experimental data by noting that to second order in the hyperfine interaction, the magnetic-field positions of the resonant lines for an $S\leq\frac{3}{2}$ spin system are given by[36]

$$B_{\rm res}=h\nu/g\beta-(\mathcal{A}_V/g)m -(\mathcal{A}_V^2/2gh\nu)[I(I+1)-m^2+m(2M-1)] , \quad (2)$$

where h is Planck's constant, ν is the klystron frequency, and M and m are the magnetic quantum numbers for the electron spin S and nuclear spin I, respectively. Equation (2) was derived on the basis of first-order selection rules, i.e., $\Delta M=\pm1,\Delta m=0$ and for the M to $M-1$ transition. An important feature of Eq. (2) is that the second-order term $(\mathcal{A}_V^2/2gh\nu)[m(2M-1)]$, although small, leads to a splitting of the hyperfine lines into $2S$ fine-structure lines. If this splitting is resolved, then a value for S can be determined by noting the number of fine-structure lines. In the present investigation of CdTe:V no fine-structure lines were observed; that is, each hyperfine should be split into two by the second-order term. It should be noted that each ^{51}V hyperfine envelope is quite broad (>20 G), which may be indicative of crystalline strains. A local monitoring of the birefringence in our sample has indeed revealed the existence of strained regions.[6] If this is the case, then it has been pointed out that the transitions $|\pm1\rangle\leftrightarrow|0\rangle$ will be broadened by the strains, whereas the double-quantum transition $|-1\rangle\leftrightarrow|+1\rangle$ will remain sharp because it is unaffected by crystalline strains in first order.[28,36] This suggests that the spectrum observed in CdTe:V may arise from double-quantum transitions, which is consistent with the observed microwave power sensitivity. The spin Hamiltonian parameters were thus obtained from the measured spectrum using a form of Eq. (2) in which the second-order term $(\mathcal{A}_V^2/2gh\nu)[m(2M-1)]$ is not included.

The ground state of V^{3+} in tetrahedral symmetry is the spin-only triplet $^3A_2$, irrespective of the strength of the crystal field. The fact that the EPR spectrum of V^{3+} is isotropic, observable at ~77 K, and microwave power sensitive near liquid-helium temperatures is consistent with the ground-state orbital singlet. Within the framework of simple crystal-field theory, the g factor for this $S=1$ state is given by[11]

$$g=g_e-8\kappa\lambda/10Dq , \quad (3)$$

where g_e is the free-electron g factor 2.0023, κ is the covalency orbital reduction factor,[37] $10Dq$ is the crystal-field parameter of V^{3+}, and λ is the effective spin-orbit coupling constant. Using reasonable estimates for the parameters in Eq. (3), i.e., $\kappa\approx0.6$, free-ion spin-orbit coupling constant $\lambda_0\approx104$ cm^{-1},[37] and therefore $\lambda\approx\kappa\lambda_0\approx73$ cm^{-1}, the predicted value of the crystal-field parameter for V^{3+} in CdTe is $10Dq\approx6300$ cm^{-1}.

Superimposed on each ^{51}V hyperfine component is additional structure. Figure 5 shows on an expanded scale the $|M_I|=\frac{1}{2}$ ^{51}V hyperfine component. This well-resolved superhyperfine structure is produced by a hyperfine interaction with nearby Cd nuclei. There are two isotopes of Cd with nonzero nuclear spins, ^{111}Cd and ^{113}Cd. Both have spin $I=\frac{1}{2}$, natural abundance of 12.75% and 12.26%, respectively, and magnetogyric ratios (γ's) differing by less than 5%. Since the observed spectrum is isotropic, it is reasonable to assume that the twelve second-nearest cadmiums are all equivalent. Not all sites, however, are equivalent in nuclear spin since the odd isotopes have $I=\frac{1}{2}$, whereas the even isotopes have $I=0$. This means that only 25% of the Cd nuclei will result in a nonzero hyperfine coupling. Assuming that $\gamma(^{111}Cd)=\gamma(^{113}Cd)$, the positions of the hyperfine lines will then be given by $\mathcal{A}_{Cd}m$, where $\mathcal{A}_{Cd}$ is the cadmium hyperfine splitting constant and $m=0,\pm\frac{1}{2},\pm1,\pm\frac{3}{2},\pm2,\ldots,\pm\frac{11}{2},\pm6$. The relative intensities of the lines are given by[38–40]

$$\mathcal{I}(m)=\sum_n[\mathcal{C}(2n)/2^{2n}][2n!/(n+m)!(n-m)!] , \quad (4)$$

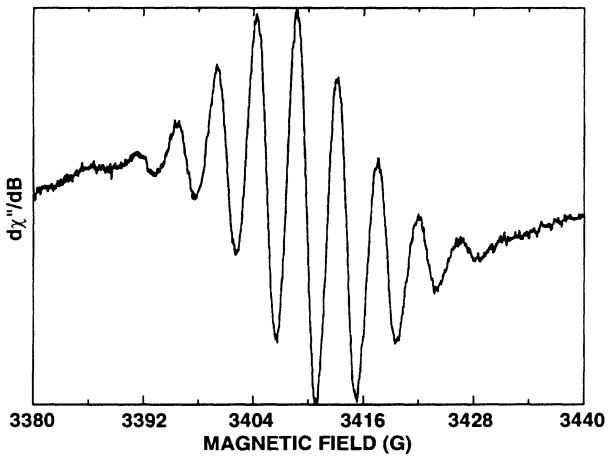

FIG. 5. EPR spectrum of CdTe:V recorded at 4.4 K showing on an expanded scale the $|M_I|=\frac{1}{2}$ ^{51}V hyperfine component. The external magnetic field $\mathbf{B}_0$ is parallel to the [001] direction. The instrumental parameters are microwave frequency $\nu=9.267\,13$ GHz, microwave power ~0.8 mW, and modulation amplitude $=2$ G.

where

$$\mathcal{C}(2n)=[12!/(2n)!(12-2n)!]\mathcal{P}_{\text{odd}}^{2n}\mathcal{P}_{\text{even}}^{12-2n} . \quad (5)$$

In Eq. (4) the sum ranges from $n=|m|$ to 6 for integral values of m and for half-integral values of m, $n=|m|$ to $\frac{11}{2}$. For the probabilities of occupation, $\mathcal{P}_{\text{odd}}=\frac{1}{4}$ and $\mathcal{P}_{\text{even}}=\frac{3}{4}$. Based on these equations, the calculated intensities of the five strongest lines (i.e., $|m|=0,\frac{1}{2},1,\frac{3}{2},2$) are in the ratio 1.00:0.837:0.498:0.215:0.069. From the peak-to-peak amplitudes of the resonances shown in Fig. 5, the intensity ratios for the five strongest lines are 1.00:0.87:0.54:0.24:0.07, which are in excellent agreement with the predicted values. Within the framework of this model, the cadmium isotropic hyperfine coupling constant is two times the separation between successive superhyperfine components, or $\mathcal{A}_{\text{Cd}}=8.78$ G (8.045×10^{-4} cm^{-1}). This large value for $\mathcal{A}_{\text{Cd}}$ indicates that the $3d$ electronic wave function for $V^{3+}(3d^2)$ is more delocalized over the CdTe lattice in comparison to $Cr^{+}(3d^5)$ (Ref. 39) and $Mn^{2+}(3d^5)$.[40]

C. Optical properties

To our knowledge, neither optical-absorption nor photoluminescence data for V^{3+} in II-VI semiconductors are available. On the other hand, numerous studies have been devoted to vanadium in III-V semiconductors[27] and, in particular, we draw on the optical data related to V^{3+} in GaAs.[41,42] In GaAs:V, V^{3+} is located at the ideal Ga substitutional tetrahedral site. The observed EPR spectrum[42,43] is isotropic and is observable at temperatures ≤ 80 K, which is indicative of a $^3A_2$ ground state. Well-resolved ^{51}V hyperfine structure is not observed, however, even at low temperatures. The optical properties are dominated by the internal transition $^3A_2(^3F)\leftrightarrow{}^3T_1(^3F)$ at 1.1 eV with zero-phonon line (ZPL) at 1.008 eV.[41,42] The position of the ZPL of the weak (parity-forbidden) $^3A_2(^3F)\leftrightarrow{}^3T_2(^3F)$ transition provides a value for the crystal-field strength $10Dq=5960$ cm^{-1}.[41] This is to be compared with the value $10Dq\approx6300$ cm^{-1} predicted from the g-factor shift [see Eq. (3)] for V^{3+} in CdTe. It is reasonable to assume that in CdTe the optical properties of V^{3+} will also be dominated by the internal transition $^3A_2(^3F)\leftrightarrow{}^3T_1(^3F)$. Then based on the similarities of the $10Dq$ values in the two hosts, it is expected that the dominant absorption band for V^{3+} in CdTe should be in the 1–1.2-eV range. Referring to Fig. 2 it is clear that this absorption will occur in the region of strong absorption corresponding to the $^4T_1(^4F)\rightarrow{}^4T_1(^4P)$ transition of the V^{2+} ion and, therefore, depending on factors such as concentration, oscillator strength, and Fermi-level position, may be obscured. It is interesting to note that optical-absorption studies of vanadium-doped GaAs in which both V^{2+} and V^{3+} spectral features are simultaneously present are consistent with the discussion given above.[44,45]

D. Absence of V^{2+} EPR in CdTe

In this section we first review the work on V^{2+} in II-VI and III-V semiconductors and then use this information to provide some insight into why it is reasonable that the EPR of V^{2+} is not observed in CdTe:V. An obvious simple explanation is that the concentration of V^{2+} is too low to be detected by EPR. This seems to contradict the observation that the optical-absorption spectrum in CdTe:V is dominated by the V^{2+} ion. It should be pointed out, however, that the optical data were recorded at room temperature; whereas due to spin-relaxation effects, the EPR measurements were carried out at low temperatures. It is well known in semiconductor physics that for a material containing both intrinsic as well as extrinsic defects (impurities), the Fermi-level position is determined by the defect number densities, ionization level positions relative to the band edges, and temperature. Thus it is possible to move the Fermi level with temperature to a position for which the V^{2+} population is much smaller than that of V^{3+}. We will address this problem in more detail in the next section. For the remainder of this section we will assume that the V^{2+} concentration is large enough to be detected by a high-sensitivity EPR spectrometer.

The only reported EPR for the V^{2+} ($3d^3$) ion in a II-VI semiconductor is that in cubic ZnS.[34] To account for the observed EPR spectrum, Schneider, Dischler, and Räuber[34] propose that the V^{2+} ion undergoes a spontaneous trigonal distortion, as a consequence of the Jahn-Teller effect,[26] along the four $\langle 111\rangle$ axes of the cubic host. This is a reasonable expectation since the ground state of the V^{2+} ion in a T_d crystalline field is an orbital triplet $^4T_1$. The degeneracy of this orbital triplet is removed by the trigonal distortion into a low-lying orbital singlet $^4\hat{A}_2$ and a higher-lying orbital doublet $^4\hat{E}$ (careted irreducible representations refer to the C_{3v} symmetry group). The g factors and ^{51}V hyperfine coupling constants for V^{2+} in ZnS are listed in Table I.

It is also instructive to examine the work on Cr^{3+}, likewise a $3d^3$ ion, in semi-insulating GaAs:Cr.[46] In this host the Cr^{3+} EPR spectrum is only easily observed for temperatures below 5 K; at higher temperatures (>10 K) the spectrum is broadened beyond detection. In order to explain these observations, Krebs and Stauss[46] suggest that the Cr^{3+} ion in GaAs, which has an orbital triplet ground state $^4T_1$, undergoes an orthorhombic distortion (there are six equivalent static orthorhombic states) attributed to a strong Jahn-Teller effect. Above 5 K the Cr^{3+} center (including its four ligands) rapidly reorients between the six possible equivalent orthorhombic distortions. This rapid motion leads to broadening of the spectrum; at still higher temperatures, however, where motional narrowing should be expected,[47] the signal intensity is too weak to be observed because of possible spin-lattice relaxation effects.[11,47]

The V^{2+} ion has also been studied extensively in GaAs. First-principles spin-polarized Green-function calculations by Katayama-Yoshida and Zunger[48] for substitutional vanadium predict a ^2E low-spin ground state, rather than the normally expected (according to Hund's rule) high-spin $^4T_1$ state. Both optically detected[42] and thermally detected[49–51] paramagnetic resonance provide evidence for this unusual assignment of the ground state. What tends to be somewhat incompletely resolved by these studies is whether the vanadium center in GaAs is

an isolated substitutional center, i.e., V^{2+} at a gallium site without any near-neighbor defect. However, the most recent thermally detected EPR study[52] of vanadium-doped GaAs indicates that two V^{2+} centers are present; one corresponding to an isolated substitutional V^{2+} with a ^2E ground state, and the other assumed to be part of a complex, labeled as $V^{2+}(II)$, with a $^4T_1$ ground state.

It is clear from the discussion above that $3d^3$ ions such as Cr^{3+} and V^{2+} can be stabilized in GaAs and ZnS. These ions have in T_d-crystalline fields, however, orbitally degenerate ground states which can experience dynamic Jahn-Teller configurational distortions. Evidence for the presence of V^{2+} in CdTe:V is provided by the optical-absorption spectrum (Fig. 2). It is reasonable to expect that the V^{2+} ion in CdTe:V will have an orbital degenerate ground state with either $^4T_1$ high-spin symmetry (in accordance with Hund's rule) or possibly low-spin ^2E symmetry. Therefore, assuming that the concentration level is favorable for EPR detection, we suggest that a dynamic Jahn-Teller effect[26] may be operative which manifests itself in the broadening of the V^{2+} EPR spectrum beyond detection.

E. Photo-EPR

Before discussing the results of the photo-EPR measurements we first examine in more detail the internal optical transitions of the V^{2+} ion in CdTe:V. As shown in Fig. 4, the excited crystal-field states for the V^{2+} ion in CdTe:V, i.e., the $^4A_2(^4F)$, $^2E(^2G)$, and $^4T_1(^4P)$ states, penetrate into the CdTe host conduction band. Since it is highly probable for these localized excited ion states to be degenerate with the extended electronic (Bloch) states of the host crystal, it is reasonable to assume that the internal $d \rightarrow d^*$ transitions will contribute to the photoconductivity[14] through self-ionization channels formed by the coupling between the localized and extended states.[52] For this single-donor photoionization process, V^{2+} is converted to V^{3+} with an electron in the conduction band and one of the possible channels is represented by the following reaction:[25]

$$[V^{2+},(CB)^0,^4T_1(^4F)] \rightarrow [V^{3+},(CB)^1,^3A_2(^3F)] , \quad (6)$$

or more physically by

$$V^{2+} + h\nu \rightarrow V^{3+} + e_{CB}^- . \quad (7)$$

In the above equations $(CB)^0$ and $(CB)^1$ refer to the occupation of the conduction-band minimum and e_{CB}^- represents an electron in the conduction band. If this photoionization process occurs, then the above reactions predict that the V^{3+} concentration should increase under illumination with 1.319-nm (0.94 eV) light. This is not consistent with what is observed, and therefore other photophysical pathways must be explored.

One possible route leading to a reduction of the V^{3+} population under sub-band-gap illumination involves hole ionization and is described by the following reaction:

$$V^{3+} + h\nu \rightarrow V^{2+} + h_{VB}^+ , \quad (8)$$

where h_{VB}^+ corresponds to a hole in the valence band. This channel appears to be inconsistent with the photorefractive results which imply that the carriers are electrons. However, in contrast with the photorefractive measurements which are carried out at room temperature, the photo-EPR measurements are carried out at low temperatures because of spin-lattice relaxation effects. As the temperature is lowered in CdTe:V, changes in the concentration of V^{2+} and V^{3+} ions, and the electron or hole optical generation rates, are expected.

The undoped CdTe as grown by our method usually exhibits p-type conductivity. It is believed that the role of vanadium dopant is to compensate for shallow levels which, in turn, results in semi-insulating properties. It is possible that due to changes in the thermal generation/recombination rates of shallow defects at lower temperatures, the Fermi level can shift below the (V^{2+}/V^{3+}) ionization level where the dominant charge state of vanadium is V^{3+}. As briefly indicated in Sec. III B, the luminescence at 1.496 eV has been assigned to an optical transition terminating on a deep acceptorlike level associated with a complex center. The exact nature of this center is still not known, however experimental evidence supports the view that it is the vacancy-donor complex $(V_{Cd}^{2-}D^+)$ located about 0.14 to 0.17 eV above the valence band.[18] Since defect centers such as these or even more simple intrinsic defects including interstitial and vacancy centers are known to strongly influence the electrical and optical properties of both undoped as well as doped CdTe,[18] it is important to consider their role in the present study. In particular, for the case where the number density of shallow acceptors is much greater than that of shallow donors ($[A] \gg [D]$), then the following photophysical channel is relevant:

$$V^{3+} + A^- + h\nu \rightarrow V^{2+} + A^0 , \quad (9)$$

where A^- and A^0 represent ionized and neutral acceptors, respectively. Equation (9) predicts a reduction of the V^{3+} population under sub-band-gap illumination. As discussed above, lower temperatures may lead to a shift of the Fermi level towards the valence band, which in turn leads to an increase in the population of A^-.

In addition, it should be noted that carrier emission rates, which are proportional to optical cross sections for the respective carriers, could be strongly temperature dependent.[53] Therefore, it is possible that at lower temperatures, hole emission from the (V^{2+}/V^{3+}) level is favored over electron emission as described by Eq. (8). Preliminary optical-absorption measurements at low temperatures reveal spectral features that are notably different from that observed at room temperature. Limitations on sample size and surface quality, as well as experimental setup, have precluded a complete spectral analysis of the data; however, these changes in the absorption spectrum are consistent with our view regarding a possible change in the number density of V^{2+} and V^{3+} ions and/or carrier emission rates for the (V^{2+}/V^{3+}) ionization level.

V. SUMMARY AND CONCLUSIONS

In this study we have investigated photorefractive vanadium-doped CdTe by EPR, photo-EPR, optical ab-

sorption, and photoluminescence spectroscopies. We report the EPR of the V^{3+} ion on CdTe. Contrary to our expectation, the EPR of V^{2+} was not observed. The optical-absorption spectrum recorded at room temperature on the sample measured by EPR, however, shows internal transitions assigned to the V^{2+} ion. Photo-EPR measurements demonstrate that the V^{3+} ion in CdTe:V is optically active at 1.32-μm wavelength (sub-band-gap illumination). Mechanisms to account for the decrease in the EPR of the V^{3+} signal under sub-band-gap illumination have been presented. Since EPR measurements are made at low temperatures, whereas photorefractive studies are carried out at room temperature, a complete correlation between the measurements was not possible. However, these measurements provide direct evidence that the deep level associated with the vanadium dopant is involved in the photoionization process in CdTe:V. Contrary to other views[8] regarding the role of vanadium in CdTe, this study provides definite evidence of vanadium substitutional incorporation and optical activity in this photorefractive material.

A paper by H. J. von Bardeleben, J. C. Launay, and V. Mazoyer [Appl. Phys. Lett. **68**, 1140 (1993)] has recently appeared that reports EPR data on the V^{3+} ion in CdTe:V. Their measured values for the g factor and Cd superhyperfine coupling constant differ from those reported in this paper. The discrepancy between the two reported g factors may be due to the fact that in this paper the data were analyzed using expressions for the resonance magnetic-field positions accurate to within second-order perturbation terms in the hyperfine interaction. To account for the discrepancy in the two reported Cd superhyperfine coupling constants, it should be noted that the value reported here is a factor of 2 larger than that reported by von Bardeleben *et al.* This suggests that the latter authors may not have realized that the observed separation between adjacent superhyperfine components is equal to one-half the Cd superhyperfine coupling constant, as indicated by the analysis summarized in this paper.

ACKNOWLEDGMENTS

The authors are grateful to Dr. M. B. Klein, Professor W. H. Steier, and Dr. A. Partovi for useful discussion on various aspects of the photorefractive effect in CdTe:V. The authors also acknowledge Dr. Y. Zoe and Dr. L. Chen for their assistance in carrying out the low-temperature optical measurements.

[1] *Photorefractive Materials and their Applications I and II,* edited by P. Günter and J.-P Huignard, Topics in Applied Physics Vols. 61 and 62 (Springer-Verlag, Berlin, 1989).

[2] A. M. Glass and J. Strait, in *Photorefractive Materials and their Applications I* (Ref. 1), Chap. 8, p. 237.

[3] A. M. Glass, Science **238**, 1003 (1987).

[4] R. B. Bylsma, P. M. Bridenbaugh, D. H. Olson, and A. M. Glass, Appl. Phys. Lett. **51**, 889 (1987).

[5] A. Partovi, J. Millerd, E. M. Garmire, M. Ziari, W. H. Steier, S. Trivedi, and M. B. Klein, Appl. Phys. Lett. **57**, 846 (1990).

[6] M. Ziari, W. H. Steier, P. N. Ranon, M. B. Klein, and S. Trivedi, J. Opt. Soc. Am. B **9**, 1461 (1992).

[7] M. Ziari, W. H. Steier, P. N. Ranon, S. Trivedi, and M. B. Klein, Appl. Phys. Lett. **60**, 1052 (1992).

[8] J. P. Zielinger, M. Tapiero, Z. Guelli, G. Roosen, P. Delaye, J. C. Launay, and V. Mazoyer, Mater. Sci. Eng. B **16**, 273 (1993).

[9] M. Ziari, W. H. Steier, M. B. Klein, and S. Trivedi, in *Technical Digest on Photorefractive Materials, Effects and Devices, 1991* (Optical Society of America, Washington, D.C., 1991), Vol. 14, pp. 159–161.

[10] M. Ziari, Ph.D. dissertation, University of Southern California, Los Angeles (1992).

[11] A. Abragam and B. Bleaney, *Electron Paramagnetic Resonance of Transition Ions* (Oxford University Press, London, 1970).

[12] D. T. F. Marple, J. Appl. Phys. **35**, 539 (1964).

[13] P. A. Slodowy and J. M. Baranowski, Phys. Status Solidi B **49**, 499 (1972).

[14] J. M. Baranowski, J. M. Langer, and S. Stepanova, in *Proceedings of the 11th International Conference on the Physics of Semiconductors, Warsaw* (Poland Scientific, Warsaw, 1972), p. 1008.

[15] L. M. Hoang and J. M. Baranowski, Phys. Status Solidi B **84**, 361 (1977).

[16] C. B. Norris and K. R. Zanio, J. Appl. Phys. **53**, 6347 (1982).

[17] N. C. Giles, S. Hwang, J. F. Schetzina, S. McDevit, and C. J. Johnson, J. Appl. Phys. **64**, 2656 (1988).

[18] K. Zanio, in *Semiconductors and Semimetals,* edited by R. K. Willardson and A. C. Beer (Academic, New York, 1978), Vol. 13.

[19] N. V. Agrinskaya, G. I. Aleksandrova, E. N. Arkad'eva, B. A. Atabekov, O. A. Matveev, G. B. Perepelova, S. V. Prokof'ev, and G. I. Shmanenkova, Fiz. Tekh. Poluprovodn. **8**, 317 (1974) [Sov. Phys. Semicond. **8**, 202 (1974)].

[20] W. H. Press, B. P. Flannery, S. A. Teukolsky, and W. T. Vetterling, *Numerical Recipes in C* (Cambridge University Press, Cambridge, 1988).

[21] G. C. Valley, S. M. McCahon, and M. B. Klein, J. Appl. Phys. **64**, 6684 (1988).

[22] V. S. Bagaev, T. Y. Belousova, Y. N. Berozashili, and D. S. Lordkipanidze, Fiz. Tekh. Poluprovodn. **3**, 1687 (1969) [Sov. Phys. Semicond. **3**, 1418 (1970)].

[23] A. M. Glass, M. B. Klein, and G. C. Valley, Electron. Lett. **21**, 220 (1985).

[24] J. S. Griffith, *The Theory of Transition Metal Ions* (Cambridge University Press, Cambridge, England, 1961).

[25] A. Zunger, in *Solid State Physics: Advances in Research and Applications,* edited by H. Ehrenreich and D. Turnbull (Academic, Orlando, 1986), Vol. 39, p. 276.

[26] M. D. Struge, in *Solid State Physics: Advances in Research and Applications,* edited by F. Setiz, D. Turnbull, and H. Ehrenreich (Academic, New York, 1967), Vol. 20, p. 91.

[27] B. Clerjaud, J. Phys. C **18**, 3615 (1985).

[28] W. C. Holton, J. Schneider, and T. L. Estle, Phys. Rev. **133**, A1638 (1964).

[29]J. Dieleman, in *II-VI Semiconductor Compounds,* edited by D. G. Thomas (Benjamin, New York, 1967), p. 199.
[30]H. H. Woodbury and G. W. Ludwig, Bull. Am. Phys. Soc. **6**, 118 (1961).
[31]J. Hage, J. R. Niklas, and J.-M. Spaeth, J. Electron. Mater. **14a**, 1051 (1985).
[32]B. Lambert, H. J. von Bardeleben, and B. Deveaud, J. Phys. C **18**, L707 (1985).
[33]H. H. Woodbury and G. W. Ludwig, Phys. Rev. **117**, 102 (1960).
[34]J. Schneider, B. Dischler, and A. Räuber, Solid State Commun. **5**, 603 (1967).
[35]D. E. Scaife, Aust. J. Chem. **23**, 2205 (1970).
[36]G. W. Ludwig and H. H. Woodbury, in *Solid State Physics: Advances in Research and Applications,* edited by F. Seitz and D. Turnbull (Academic, New York, 1962), Vol. 13, p. 223.
[37]J. Owen and J. H. M. Thornley, Rep. Prog. Phys. **29**, 675 (1966).
[38]T. L. Estle, G. K. Walters and M. deWit, in *Paramagnetic Resonances, Vol. I,* edited by W. Low (Academic, New York, 1963), p. 144.
[39]G. W. Ludwig and M. R. Lorenz, Phys. Rev. **131**, 601 (1963).
[40]J. Lambe and C. Kikuchi, Phys. Rev. **119**, 1256 (1960).
[41]W. Ulrici, K. Friedland, L. Eaves, and D. P. Halliday, Phys. Status Solidi B **131**, 719 (1985).
[42]A. Görger, B. K. Meyer, J. -M. Spaeth, and A. M. Hennel, Semicond. Sci. Technol. **3**, 832 (1988).
[43]U. Kaufmann, H. Ennen, J. Schneider, R. Wörner, J. Weber, and F. Köhl, Phys. Rev. B **25**, 5598 (1982).
[44]B. Clerjaud, C. Naud, B. Deveaud, B. Lambert, B. Plot, G. Bremond, C. Benjeddou, G. Guillot, and A. Nouailhat, J. Appl. Phys. **58**, 4207 (1985).
[45]A. M. Hennel, C. D. Brandt, K. Y. Ko, J. Lagowski, and H. C. Gatos, J. Appl. Phys. **62**, 163 (1987).
[46]J. J. Krebs and G. H. Stauss, Phys. Rev. B **15**, 17 (1977).
[47]A. Abragam, *Principles of Nuclear Magnetism* (Clarendon, Oxford, 1961).
[48]H. Katayama-Yoshida and A. Zunger, Phys. Rev. B **33**, 2961 (1986).
[49]M. En-Naqadi, A. Vasson, A. Vasson, C. A. Bates, and A. F. Labadaz, J. Phys. C **21**, 1137 (1988).
[50]A. -M. Vasson, A. F. Labadz, N. Tebbal, A. Vasson, A. Gaviax, and C. A. Bates, J. Phys. Condens. Matter **4**, 4565 (1992).
[51]A. -M. Vasson, A. Vasson, M. El-Metoui, N. Tebbal, and C. A. Bates, J. Phys. Condens. Matter **5**, 2553 (1993).
[52]A. M. Stoneham, *Theory of Defects in Solids* (Oxford University Press, London, 1975).
[53]J. Bourgoin and M. Lannoo, in *Point Defects in Semiconductors II,* Springer Series in Solid State Sciences Vol. 35 (Springer-Verlag, Berlin, 1983), p. 154.